Electronic Supplementary Material (ESI) for New Journal of Chemistry.

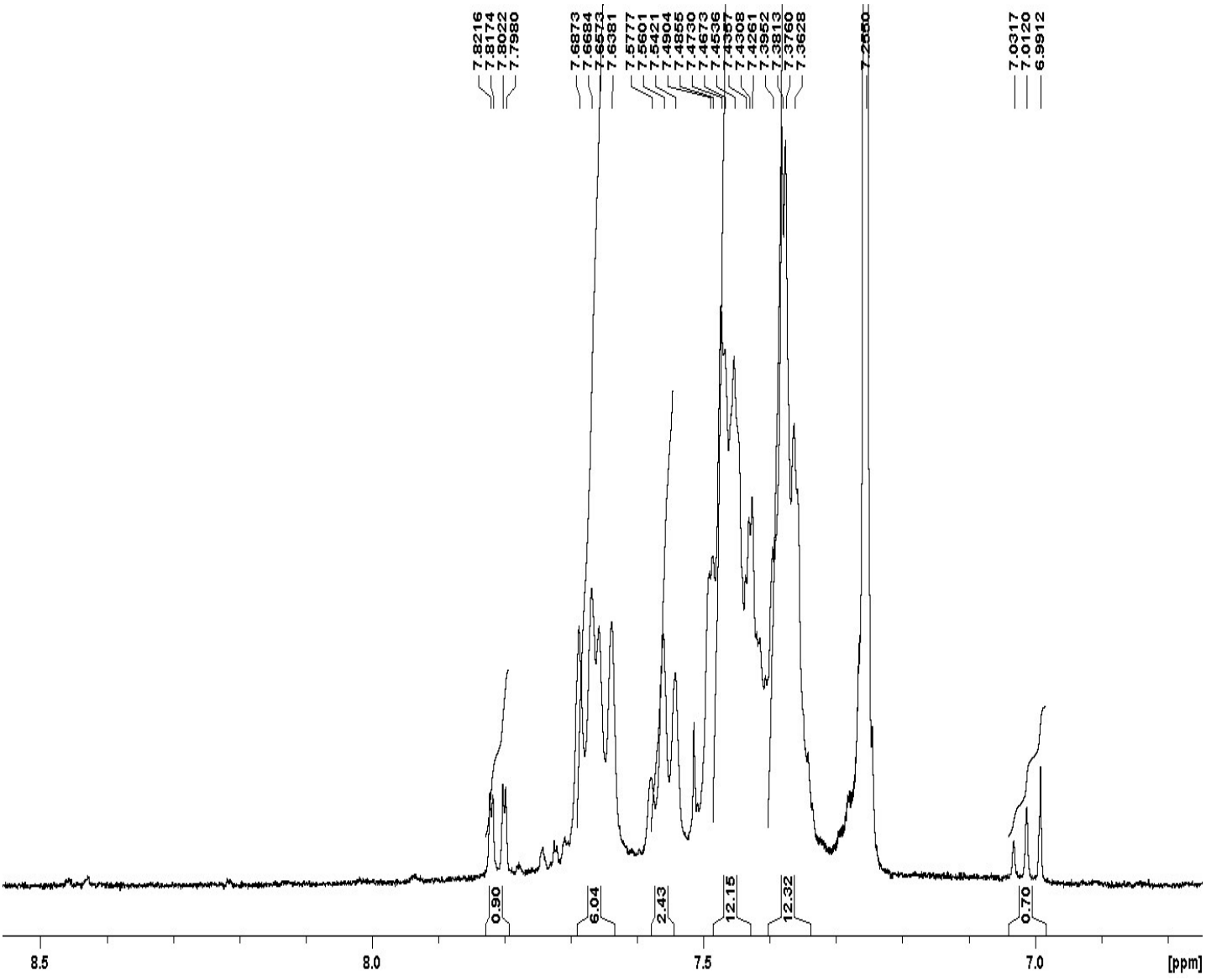

Figure 1: ^{1}H-NMR of Complex **1** in $CDCl_3$

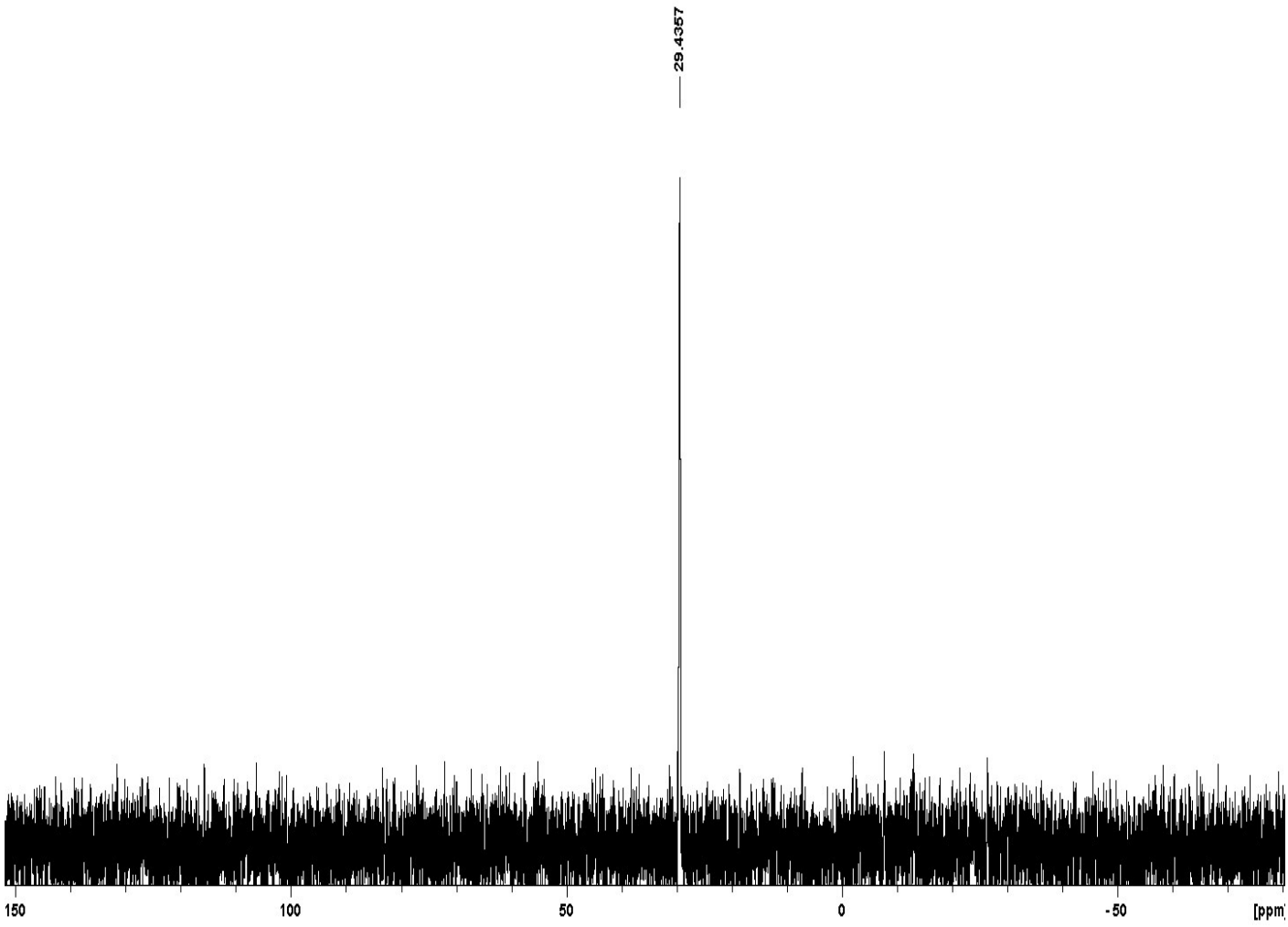

Figure 2: ^{31}P-NMR of Complex **1** in $CDCl_3$

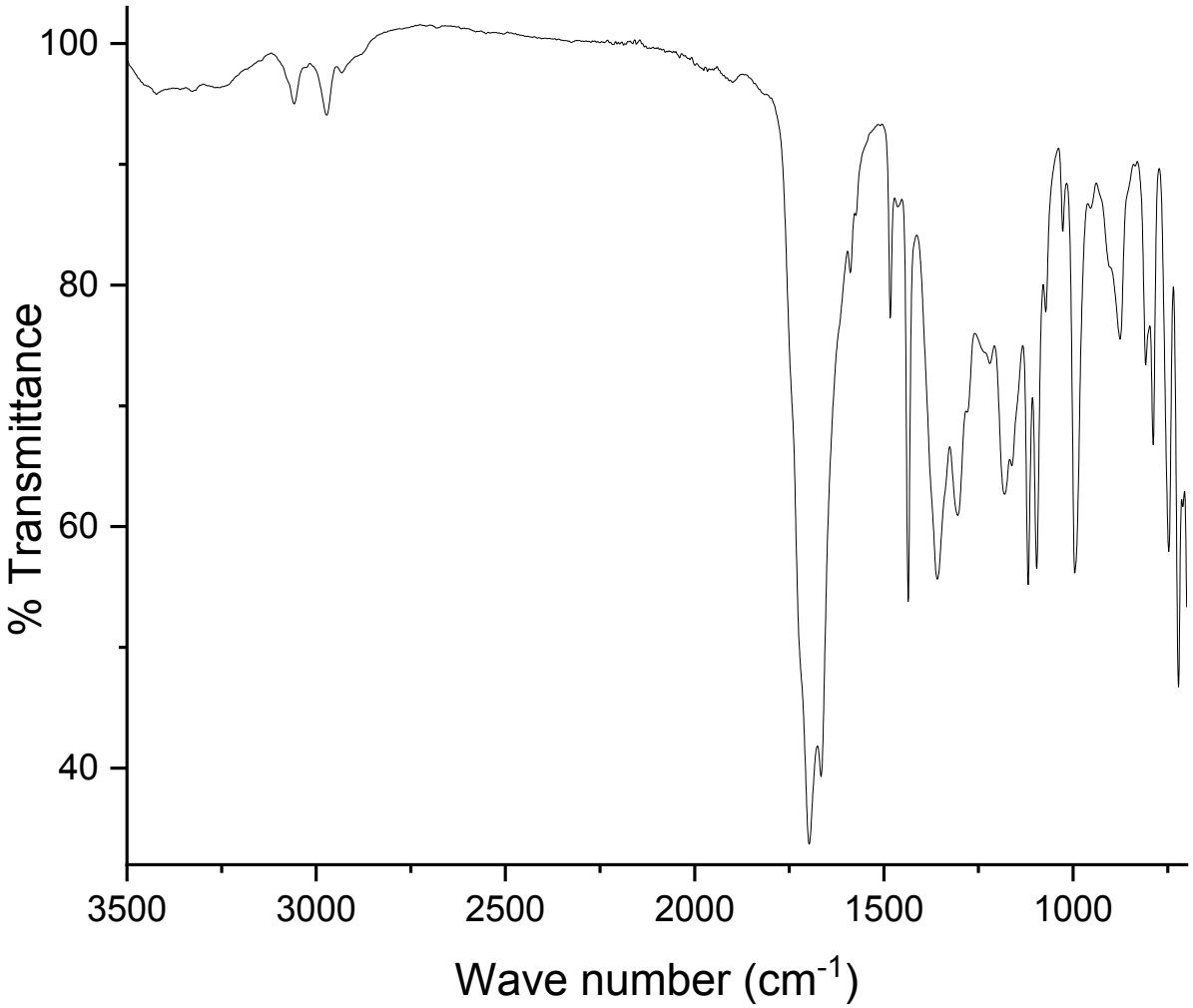

Figure 3: IR-spectrum of complex **1**

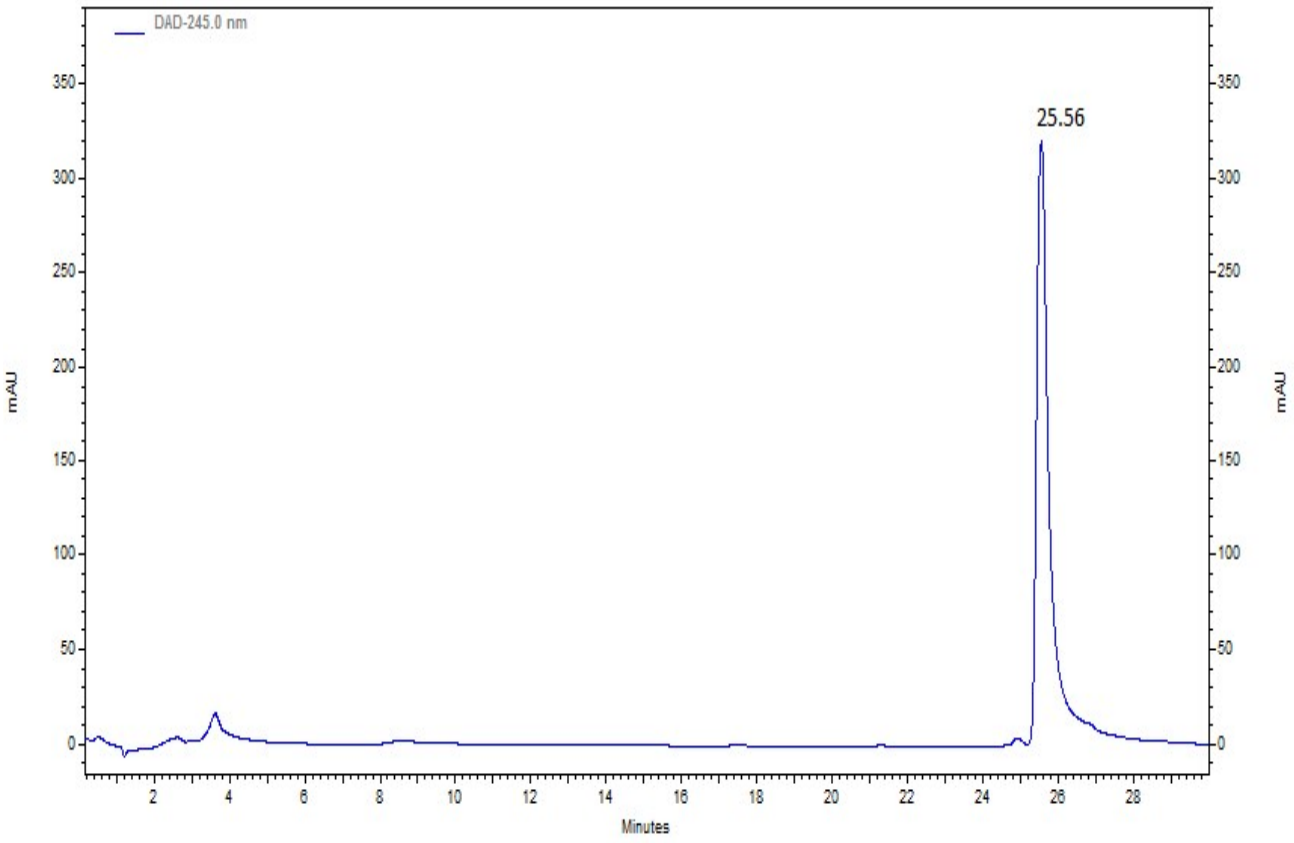

Figure 4: HPLC chromatogram of complex **1** eluted using 0.1% trifluoro-acetic acid (TFA) in H_2O (solvent A) and acetonitrile (solvent B)).

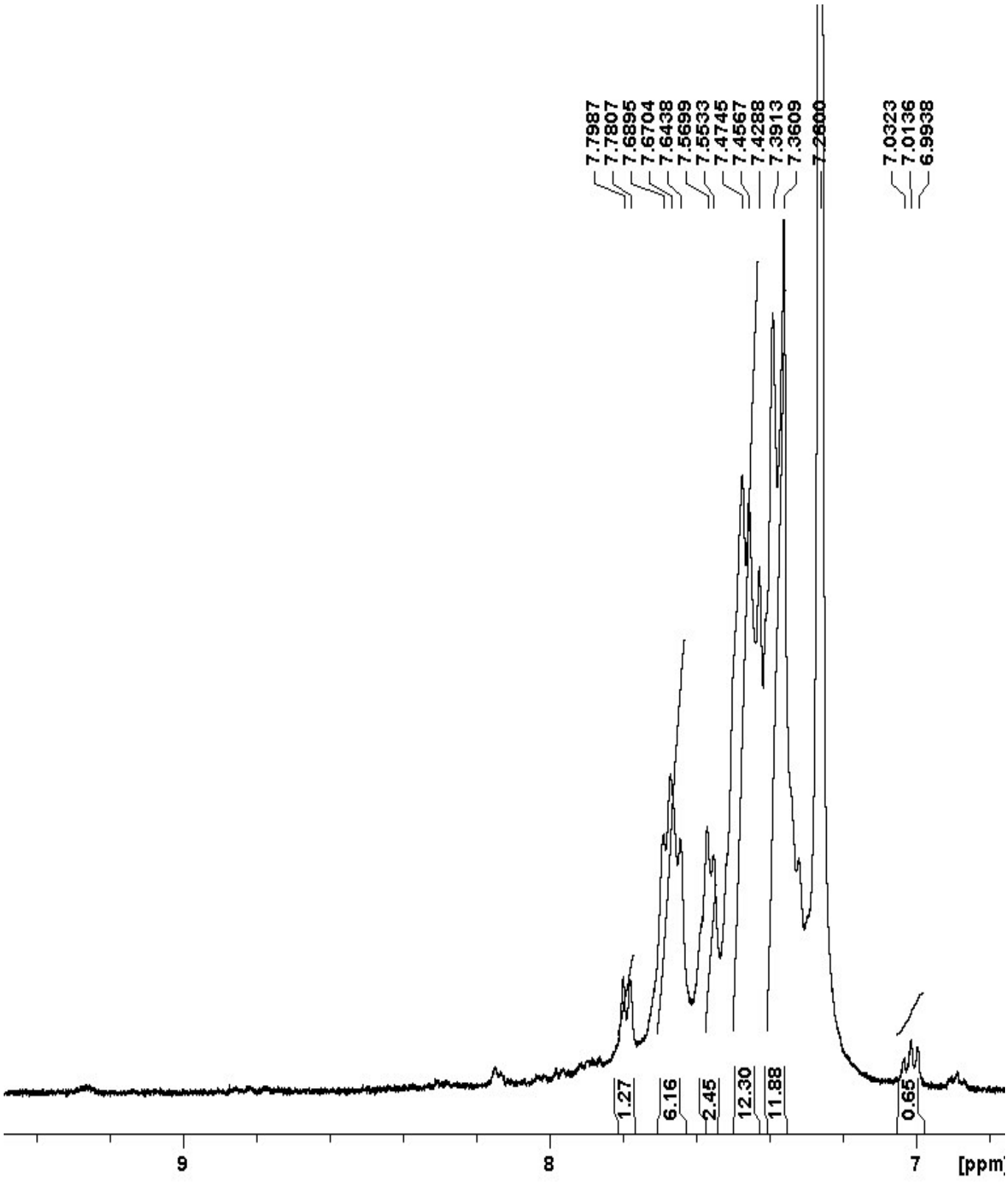

Figure 5: ^{1}H-NMR of Complex **2** in $CDCl_3$

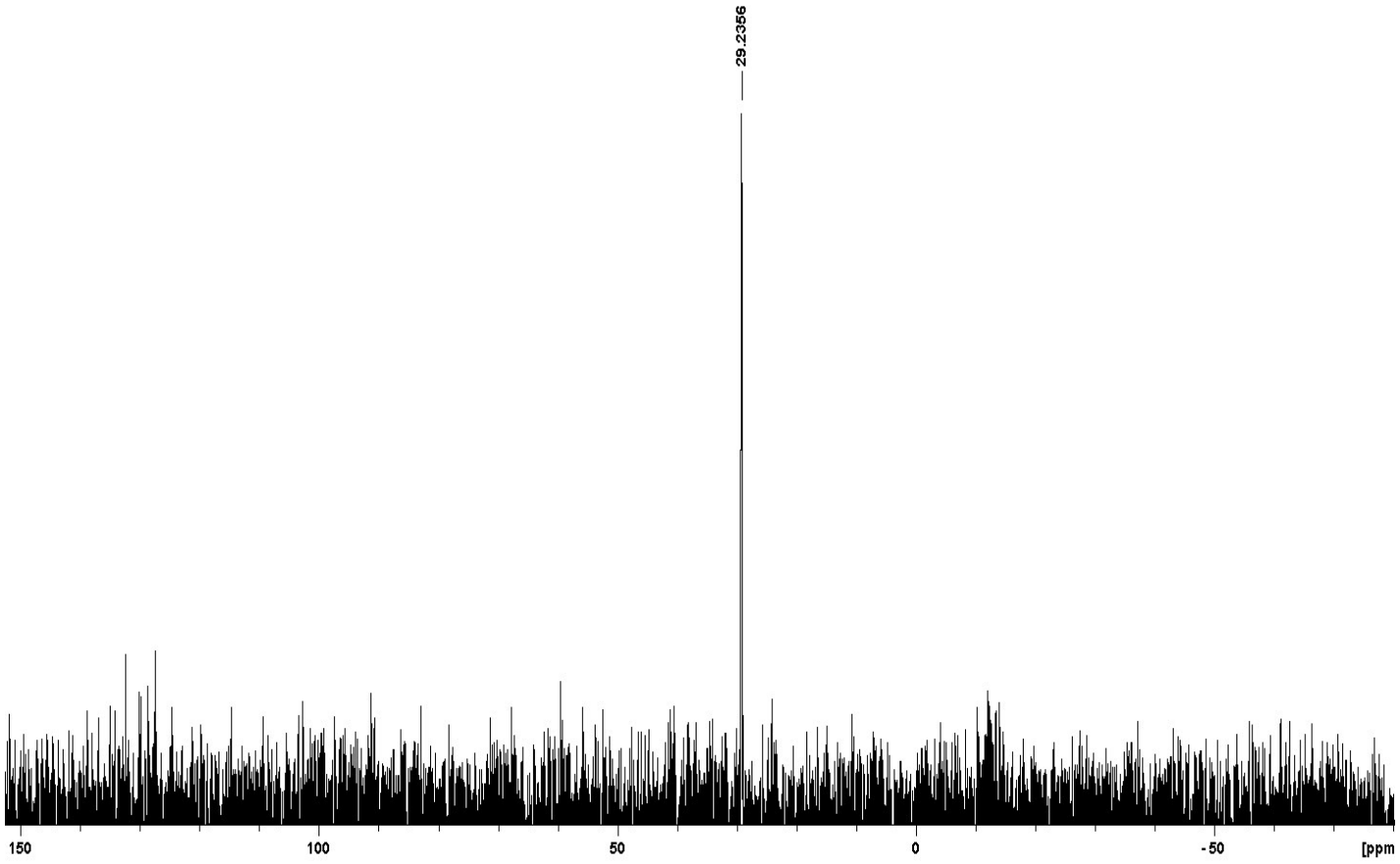

Figure 6: ^{31}P-NMR of Complex **2** in $CDCl_3$

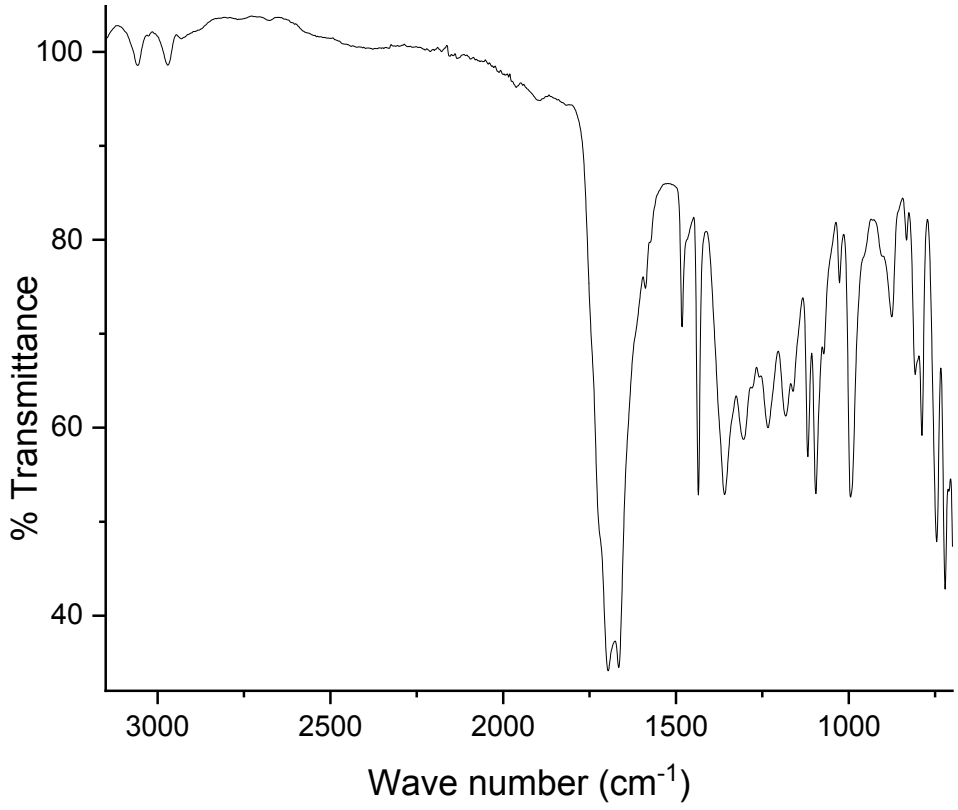

Figure 7: IR-spectrum of complex **2**

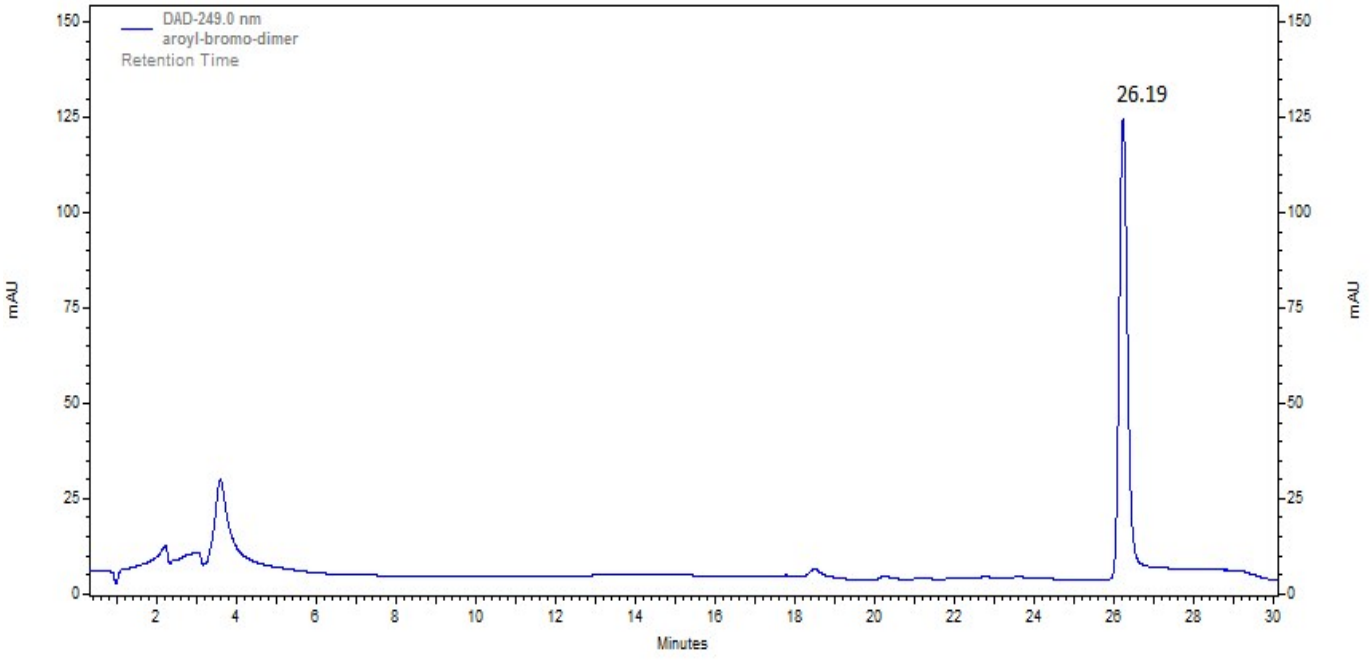

Figure 8: HPLC chromatogram of complex **2** eluted using 0.1% trifluoro-acetic acid (TFA) in H_2O (solvent A) and acetonitrile (solvent B))

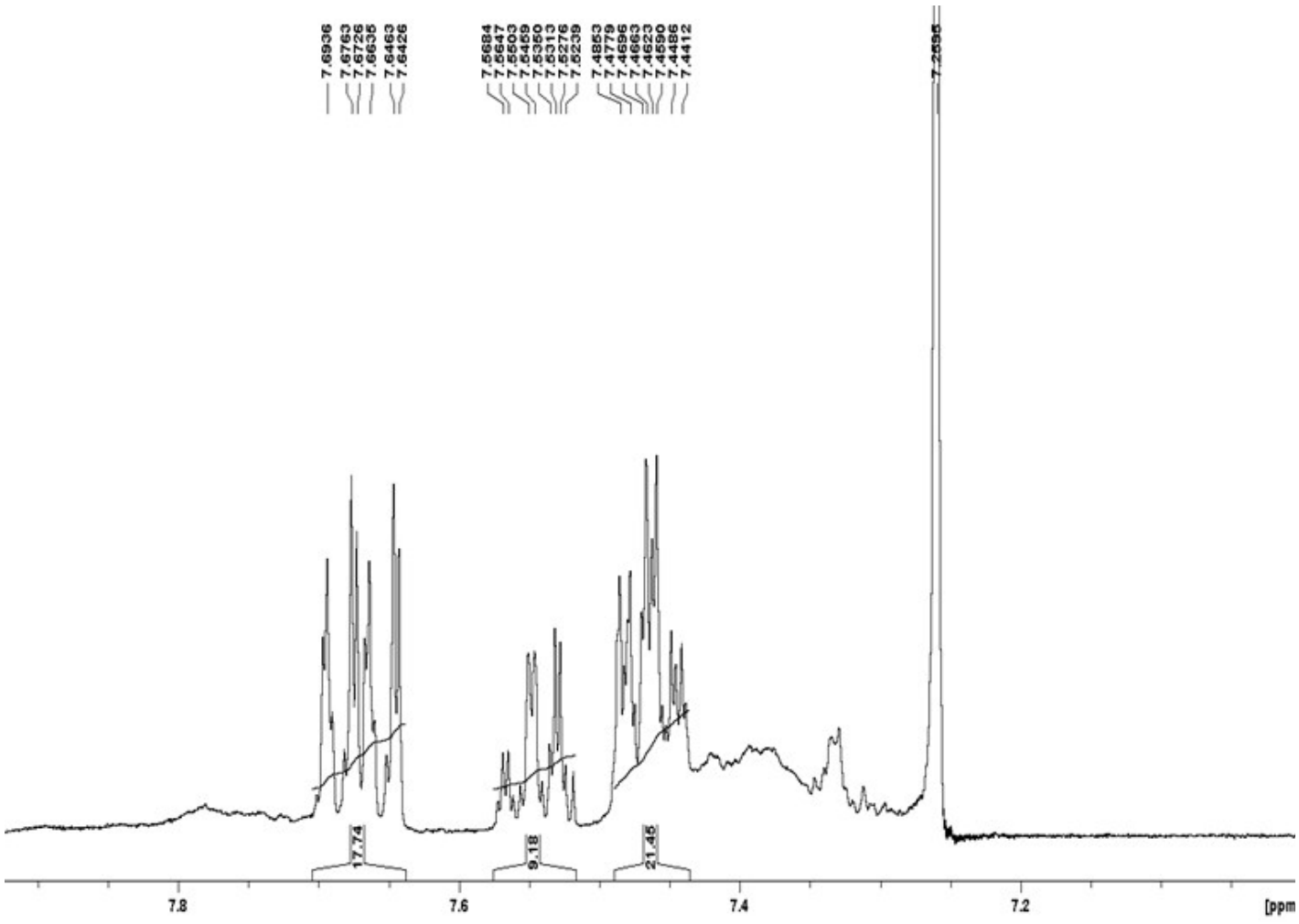

Figure 9: ^{1}H-NMR of Complex **3** in $CDCl_3$

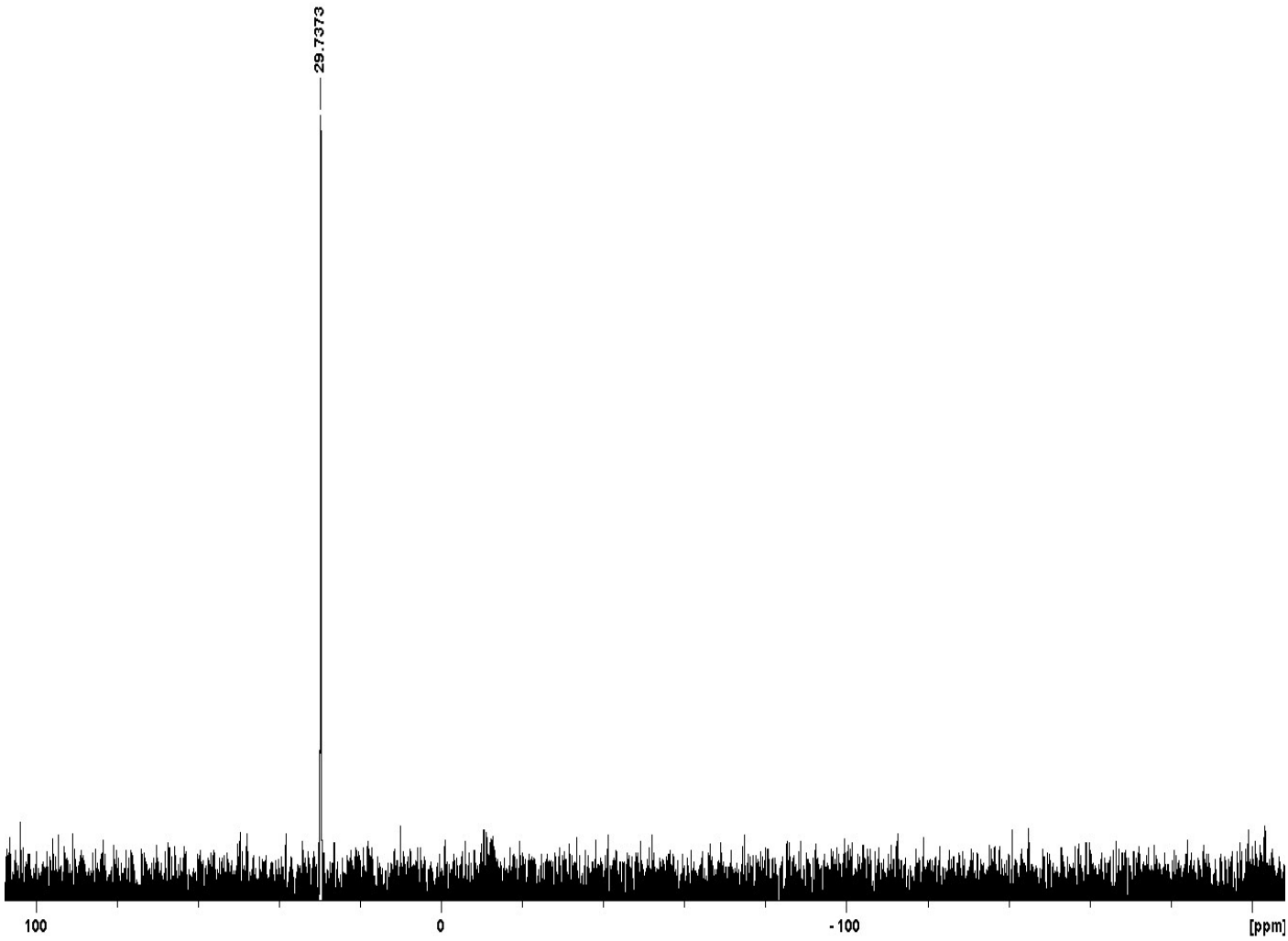

Figure 10: ^{31}P-NMR of Complex **3** in $CDCl_3$

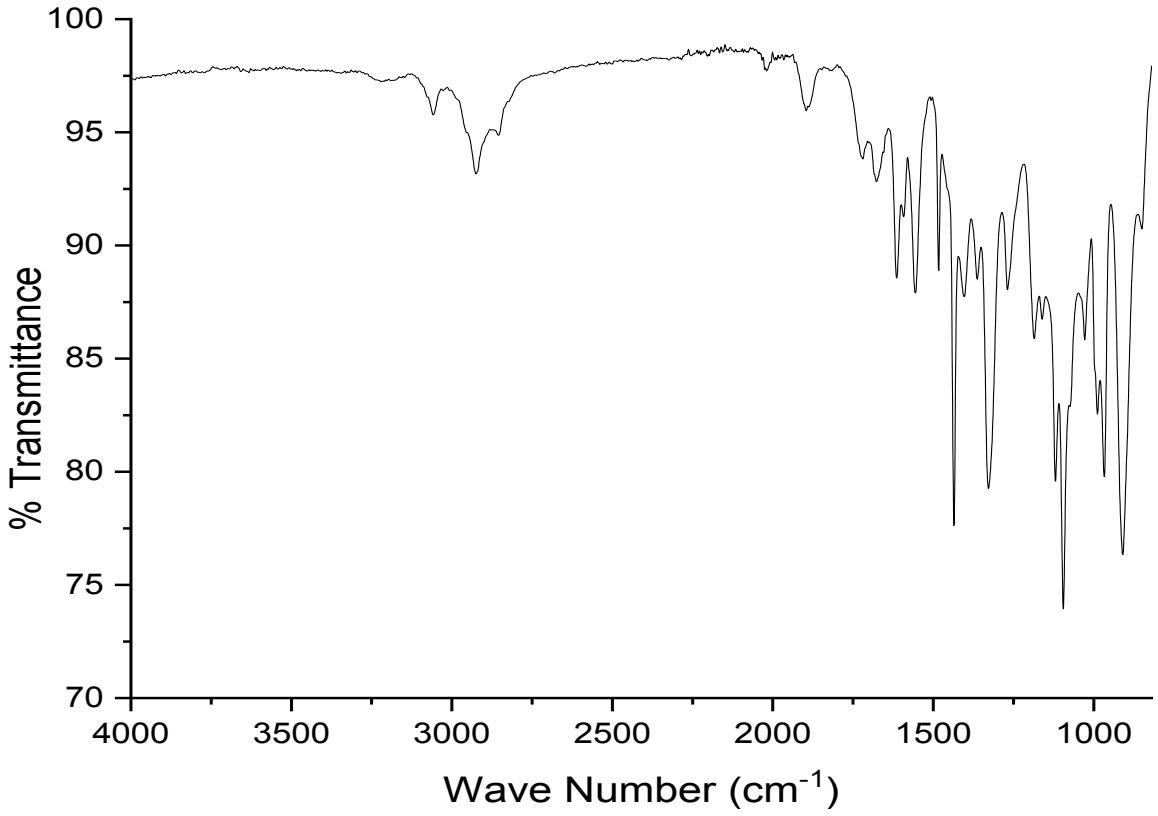

Figure 11: IR-spectrum of complex **3**

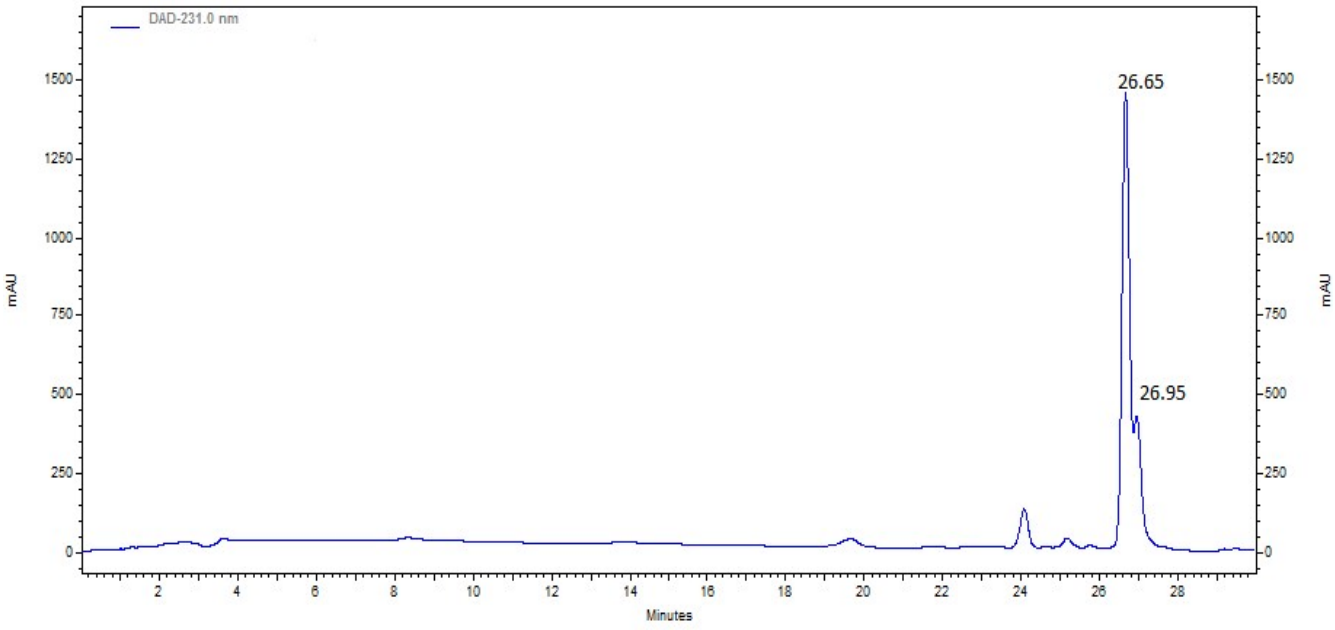

Figure 12: HPLC chromatogram of complex **3** eluted using 0.1% trifluoro-acetic acid (TFA) in H_2O (solvent A) and acetonitrile (solvent B))

The HOMO-LUMO gap provides an accurate and deep understanding about the reactivity of the molecule, and also gives an insight about the active site which is demonstrated by the distribution of frontier orbitals [39]. As HOMO-LUMO gap is low, the excitation energies for an electron from HOMO to the LUMO decreases implying the low dynamic stability, high electrical conductivity and chemical reactivity [40, 41]. The active site which is the chemical reactivity region for **1** and **2** is demonstrated by the distribution of frontier orbitals HOMO and LUMO, and they are symmetrically distributed in **1** and **2** (Fig. 13).

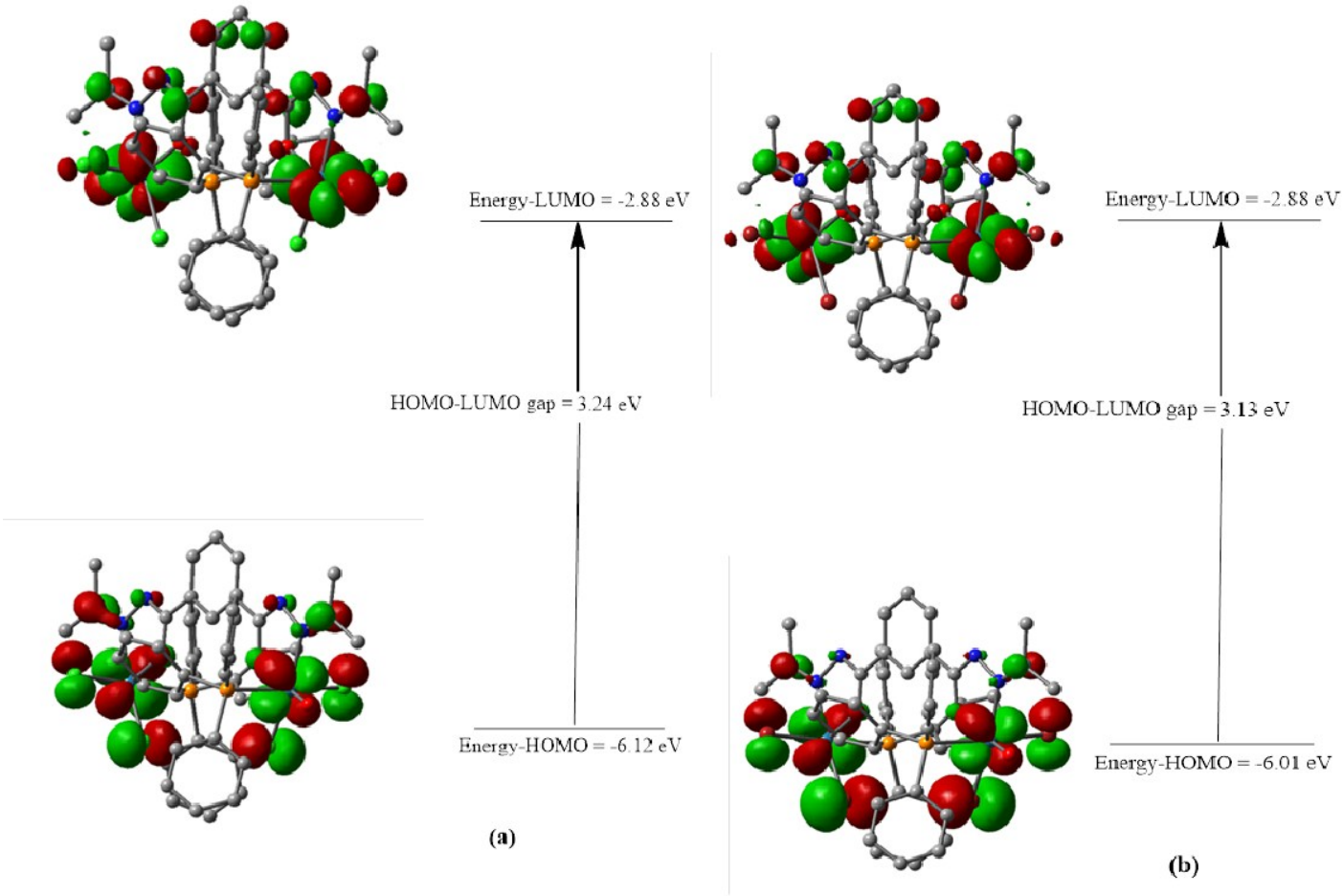

Figure 13. Spatial plots of selected frontier orbitals (HOMO and LUMO) of the DFT optimized ground state of **1** (**a**) and **2 (b)**.

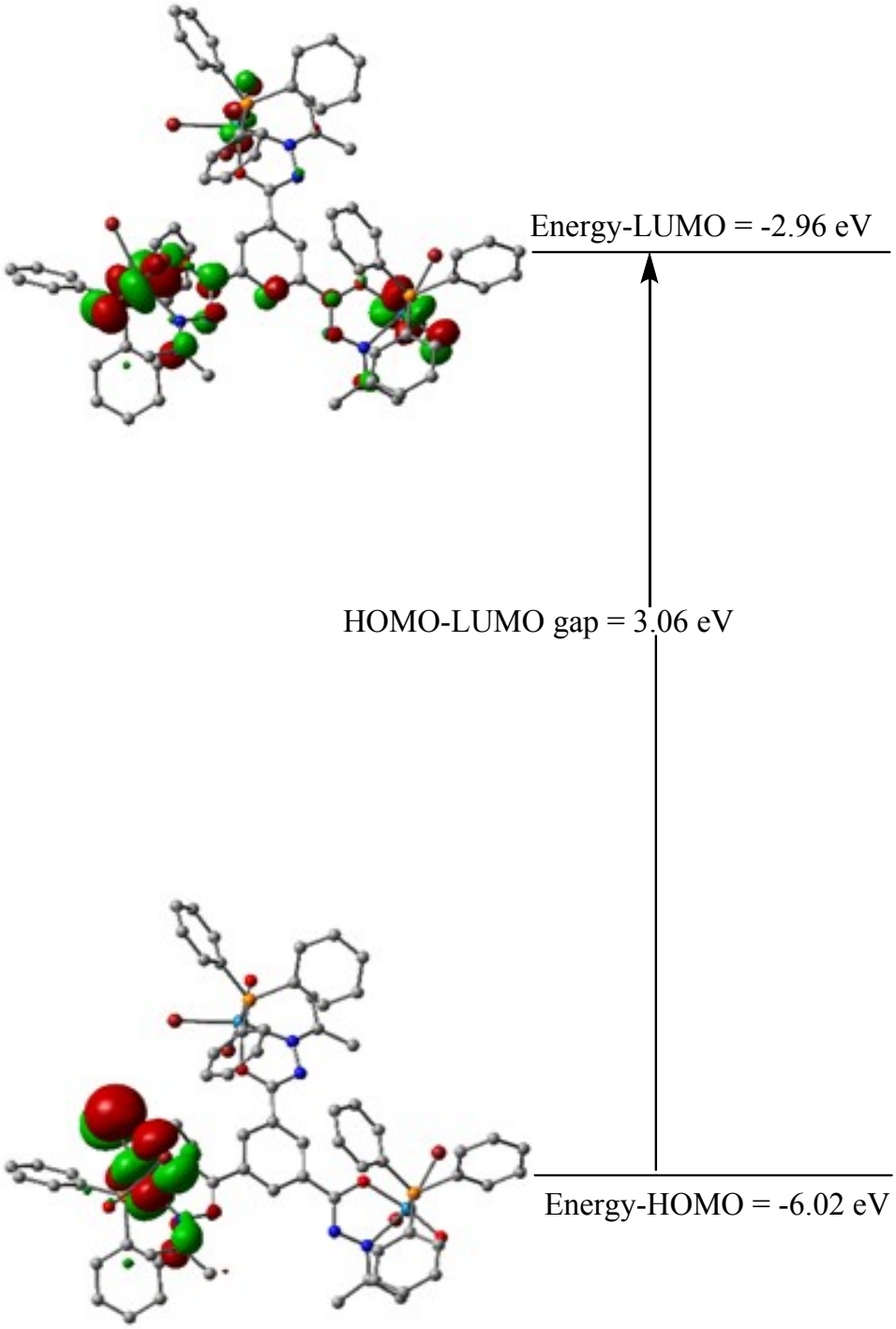

Figure 14. Spatial plots of selected frontier orbitals (HOMO and LUMO) of the DFT optimized ground state of **3**.

For evaluating the orbital energy level behavior of **3**, the first and second highest occupied molecular orbitals (HOMO-1 and HOMO-2) and lowest unoccupied molecular orbitals (LUMO+1 and LUMO+2) energy levels are calculated and they are -6.10 eV, -6.12 eV,-2.93 eV and -2.88 eV for HOMO-1, HOMO-2, LUMO+1 and LUMO+2 respectively. The HOMO-1, HOMO-2, LUMO+1 and LUMO+2 orbitals distribution are shown in Figure 8 and they are not symmetrically distributed.

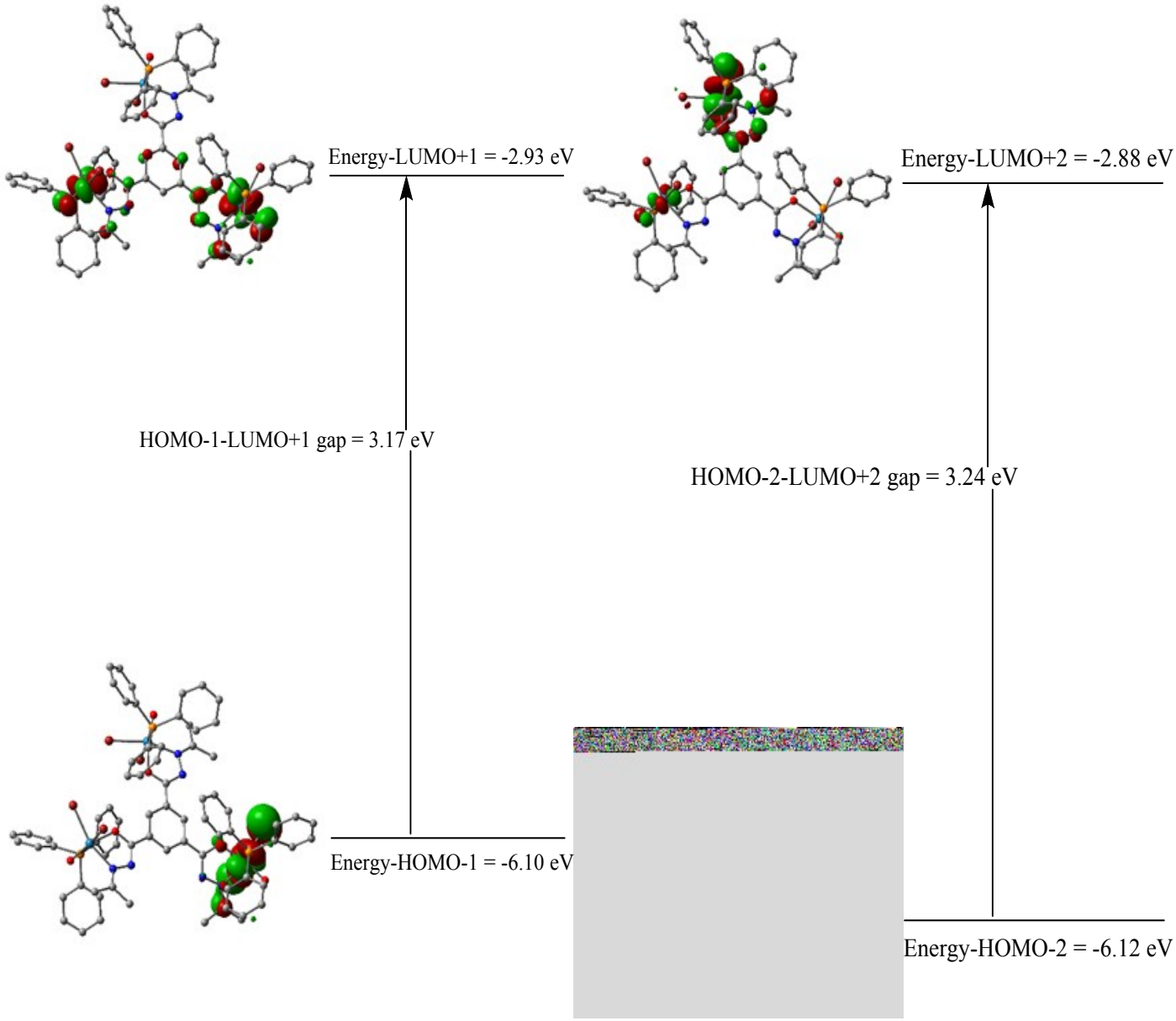

Figure 15. Spatial plots of selected frontier orbitals of the DFT optimized ground state of **3** for HOMO-1, HOMO-2, LUMO+1 and LUMO+2

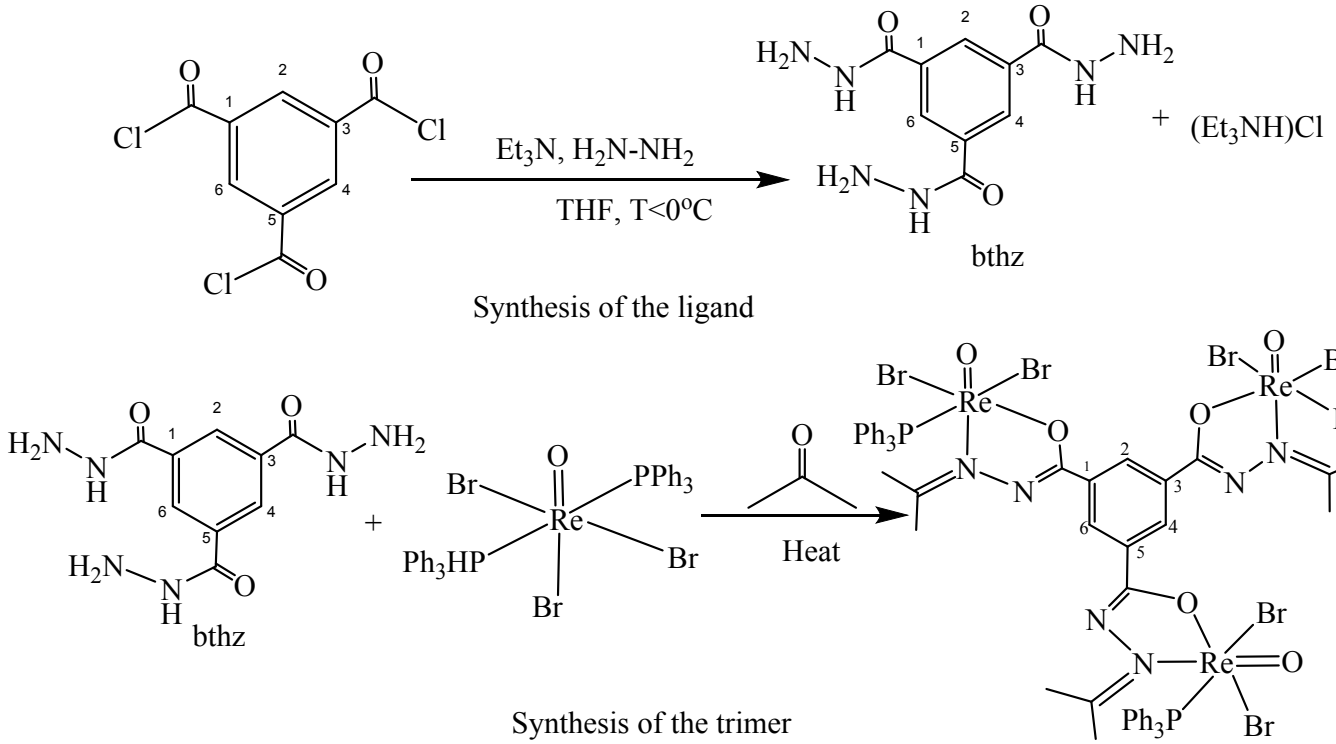

Scheme1. Synthesis of bthz and trinuclear complex 3

In the synthesis procedure of tripodal aroylhydrazine benzene-1,3,5-tricarbohydrazide (bthz) , there is $(Et_3NH)Cl$ which is formed as by-product and is held with bthz *via* hydrogen bonds, and Cl^- anion from $(Et_3NH)Cl$, compete with Br^- anion from the rhenium starting material. As a result, the chlorido-ligands are disordered with bromido-ligands in the synthesis of trinuclear complex **3** (Scheme 1).